Curr Osteoporos Rep (2013) 11:136–146
DOI 10.1007/s11914-013-0140-9

IMAGING (T LANG, SECTION EDITOR)

# High-Resolution Peripheral Quantitative Computed Tomography for the Assessment of Bone Strength and Structure: A Review by the Canadian Bone Strength Working Group

**Angela M. Cheung · Jonathan D. Adachi · David A. Hanley · David L. Kendler · K. Shawn Davison · Robert Josse · Jacques P. Brown · Louis-Georges Ste-Marie · Richard Kremer · Marta C. Erlandson · Larry Dian · Andrew J. Burghardt · Steven K. Boyd**

Published online: 24 March 2013


**Abstract** Bone structure is an integral determinant of bone strength. The availability of high resolution peripheral quantitative computed tomography (HR-pQCT) has made it possible to measure three-dimensional bone microarchitecture and volumetric bone mineral density in vivo, with accuracy previously unachievable and with relatively low-dose radiation. Recent studies using this novel imaging tool have increased our understanding of age-related changes and sex differences in bone microarchitecture, as well as the effect of different pharmacological therapies. One advantage of this novel tool is the use of finite element analysis modelling to non-invasively estimate bone strength and predict fractures using reconstructed three-dimensional images. In this paper, we describe the strengths and limitations of HR-pQCT and review the clinical studies using this tool.

A. M. Cheung
Centre of Excellence in Skeletal Health Assessment, Department of Medicine and Joint Department of Medical Imaging, University Health Network, University of Toronto, Toronto, ON, Canada

J. D. Adachi
Department of Medicine, Michael G. DeGroote School of Medicine, St. Joseph's Healthcare – McMaster University, Hamilton, ON, Canada

D. A. Hanley
Department of Medicine, University of Calgary, Calgary, AB, Canada

D. L. Kendler · L. Dian
Department of Medicine, University of British Columbia, Vancouver, BC, Canada

K. S. Davison
University of Victoria, Victoria, BC, Canada

R. Josse · M. C. Erlandson
Department of Medicine, University of Toronto, Toronto, ON, Canada

J. P. Brown
Department of Medicine, Laval University, Quebec City, PQ, Canada

L.-G. Ste-Marie
Department of Medicine, Université de Montréal, Montreal, PQ, Canada

R. Kremer
Department of Medicine, McGill University, Montreal, PQ, Canada

M. C. Erlandson
Osteoporosis and Women's Health Programs, University Health Network, Toronto, Canada

A. J. Burghardt
Musculoskeletal Quantitative Imaging Research Group, Department of Radiology and Biomedical Imaging, University of California, San Francisco, San Francisco, CA, USA

S. K. Boyd (✉)
McCaig Institute for Bone and Joint Health, Department of Radiology, University of Calgary, 3280 Hospital Drive, NW, Calgary, Alberta T2N 4Z6, Canada
e-mail: skboyd@ucalgary.ca

**Keywords** High-resolution peripheral quantitative computed tomography · Bone strength · Assessment · Bone microarchitecture · Volumetric BMD · Fracture · Age · Therapy · Finite element analysis

## Introduction

High-resolution peripheral quantitative computed tomography (HR-pQCT), commercially available in the mid-2000's, is a non-invasive, low-radiation method for assessing bone microarchitecture and volumetric bone mineral density (BMD) in cortical and trabecular compartments of the distal radius and distal tibia. Its application in clinical research has increased exponentially in the past decade (Fig. 1), and has enlightened our understanding of age-related changes and sex differences in bone microarchitecture, differences in bone structure across a wide range of bone metabolic disorders, fracture risk, and the response of bone to different osteoporosis therapies. Coupled with computer-based finite element analysis (FEA) modeling, HR-pQCT also provides a newfound approach to noninvasively assess bone strength.

Currently, only one commercial HR-pQCT machine, the XtremeCT (SCANCO Medical AG, Brüttisellen, Switzerland), is able to perform scans at a resolution sufficient to measure three-dimensional human bone microarchitecture in vivo. However, research groups worldwide are working collaboratively to advance HR-pQCT post-image processing algorithms to better quantify the observed changes.

The Canadian Bone Strength Working Group is an interdisciplinary academic group established in 2007 that has interests in advancing bone strength research and education. Although HR-pQCT is currently a research tool, there is potential for its use in the clinical diagnosis and management of osteoporosis. Our group recently performed a systematic search of published literature in the adolescent and adult population up until January 31, 2013 (Medline search terms "high-resolution peripheral quantitative computed tomography" OR "HR-pQCT", no limitations). In this paper, we aim to provide a comprehensive review of the methodology, limitations, and clinical utility of HR-pQCT with an emphasis on its use to study aging and gender differences, fracture discrimination, and treatment effects.

## HR-pQCT Scanning Techniques

### Image Acquisition

#### *Patient Positioning*

As with any medical imaging device, the proper positioning of the patient is crucial to accuracy and reproducibility. The most common usage of HR-pQCT is to image the non-dominant radius and tibia in vivo. The scanner's gantry is relatively narrow and shallow (rear physical stop) only allowing the distal peripheral skeleton to be accommodated. Although rare, some individuals with large lower leg girth are not able to fit within the scanner bore.

The limb being scanned is immobilized in a carbon fiber shell (Fig. 2a). A scout view, essentially a two-dimensional x-ray scan, is obtained so that the operator can identify a precise region for the three-dimensional measurement (Fig. 2b, c, d). The standard measurement protocol utilizes the following settings: an X-ray tube potential of 60 kVp, X-ray tube current of 95 mA, matrix size of 1536×1536 and slice thickness and in-plane voxel size of 82 μm. While the reconstructed voxel size is 82 μm for the standard patient HR-pQCT protocol, the actual spatial resolution of the image is approximately 130 μm near the center of the field of view, and somewhat less off-center (140–160 μm) [1, 2•]. Consequently, structures less than 100 μm are not typically resolved from in vivo images. At each site, 110 computerized tomography slices are obtained and used to reproduce a 9.02 mm (radial or tibial length) three-dimensional image (Fig. 2e).

Because HR-pQCT uses a polychromatic X-ray source it is subject to beam hardening as well as scatter artefacts, which can significantly impact geometric and densitometric measures [3]. Daily and weekly quality control scans should be performed to identify drift, which can occur as a consequence of decreased X-ray emission (decay). The HR-pQCT single-scan effective dose is estimated to be 3 μSv [4]. Given that exposure is additive, we recommend no more than three measures at a single site during an appointment due to the recommended radiation dose limit being 50 μSv/year (International Commission on Radiological Protection).

#### *Motion Artefact*

Because HR-pQCT has a high resolution and scan times are relatively long (3 minutes), any movement during the scan can result in movement artefact, impacting the accuracy and reproducibility of the images obtained or rendering the image unusable. Measures of micro-architecture are more sensitive to movement artefact compared with geometric or densitometric measures [5–7, 8•]. While automated and well-defined manual grading techniques to quantify and correct for motion artefact have been developed [7, 8•, 9, 10], the best solution to date is to re-scan the patient as the effect of motion on parameter errors are typically not systematic and correction algorithms cannot be applied to the parameters themselves [9].

Automated motion detection does provide the possibility for real-time assessment of scan quality allowing for the operator to decide whether a re-scan is necessary [8•]. Pialat

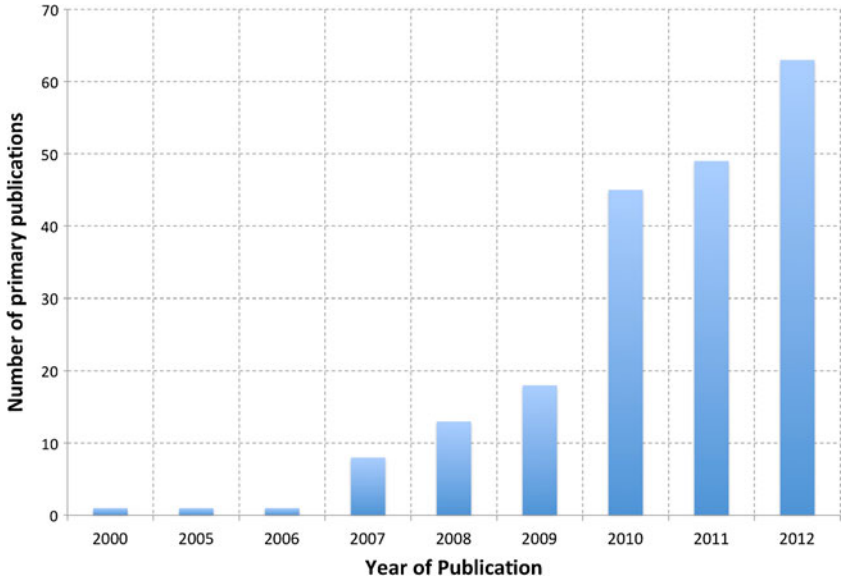


**Fig. 1** The number of publications each year that utilized high-resolution peripheral quantitative computed tomography

et al [6] reported that in 22.7 % of their scans motion artefacts necessitated a re-scan. Looking forward, improved immobilization would improve data quality and minimize the need for re-scanning.

*Image Registration*

When a patient needs to be followed longitudinally, image registration is applied to ensure the same region is consecutively assessed. The HR-pQCT system includes a default image registration that matches repeat scans by aligning similar-sized slices. More sophisticated three-dimensional registration methods have also been developed [4, 11].

## Image Analyses

Once the images have been acquired, a default patient evaluation protocol is used to analyze the scans over the entire 9.02 mm three-dimensional region to assess a wide range of standard and optional structural and density parameters, defined in Table 1 (Fig. 2d presents a typical HR-pQCT section).

*Standard Measures*

A good description of the techniques used to provide three-dimensional measures are given in Boutroy et al 2005 [12], and it is important to recognize that although these analysis methods are based on techniques developed for micro-computed tomography (μCT), some of the parameters with HR-pQCT are derived rather than directly measured (eg, trabecular thickness), because the voxel size of the scanner is close to the average thickness of a human trabecular structure [13, 14]. In future versions of HR-pQCT scanners, it may be possible to directly measure all microarchitecture parameters; however, that is not currently possible with the standard analysis protocol.

*Secondary Analyses*

The three-dimensional data from HR-pQCT offers opportunities to develop new techniques and parameters to describe and quantify the plate and rod-like structure of bone. These include structure model index [15], connectivity density (initially developed for μCT of ex vivo bone) [16, 17], and individual trabecular segmentation (ITS) [18]. Methods have also been established to improve the segmentation of the cortical and trabecular compartment [19, 20, 21•], and subsequently measure cortical parameters such as cortical porosity [21•, 22•]. There are other applications under development, such as for the visualization and quantification of bony erosions in a rheumatoid arthritis hand [23]. Certainly, these and future analyses will continue to add value to HR-pQCT measurements.

## Accuracy and Precision

The HR-pQCT systems have been thoroughly tested for both accuracy and precision using μCT of ex vivo bone as the gold-standard. Whereas accuracy is typically assessed using cadaver data, precision is based on repeated measures analyses from in vivo scanning.

*Accuracy*

There is moderate to good agreement ($r^2$=0.59–0.98) between the HR-pQCT and μCT for the assessment of cadaveric morphological parameters [1, 24–28]. Other assessments, such as connectivity density ($r^2$=0.90) [24], mechanical stiffness

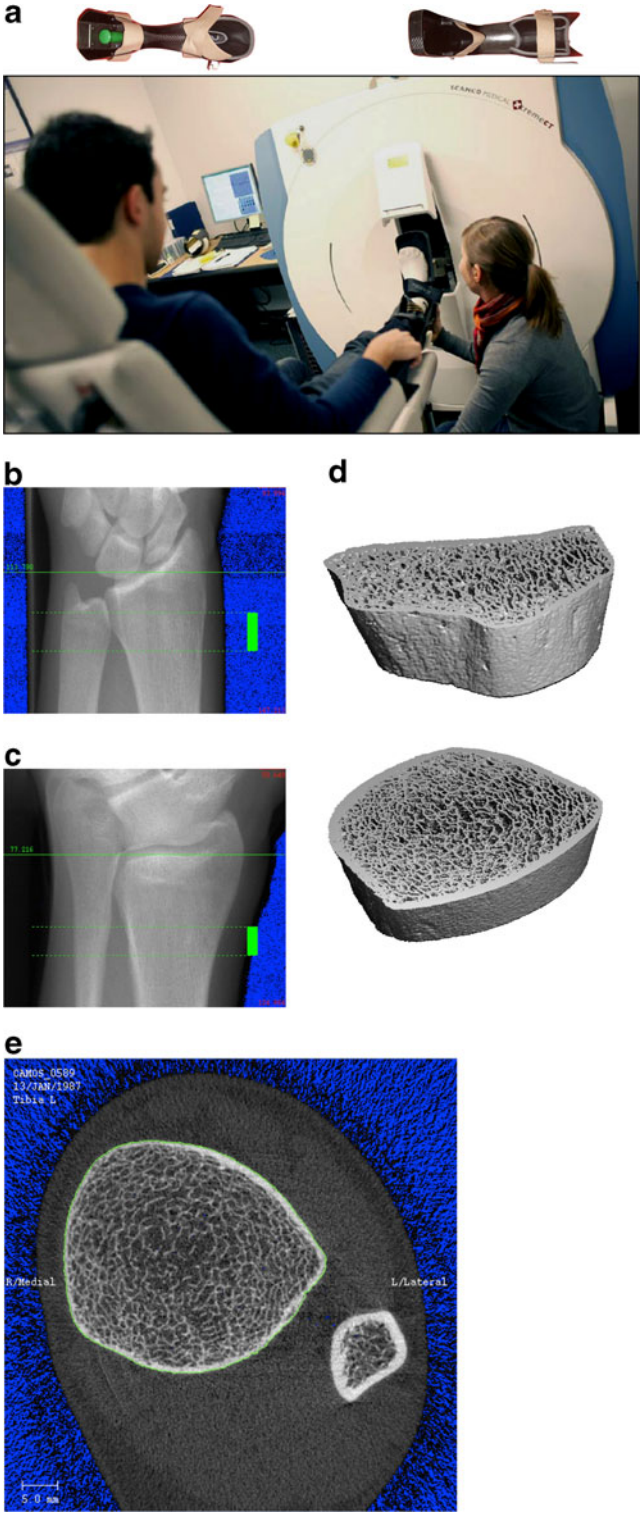


**Fig. 2** **a**, A typical setup of HR-pQCT for patient measurements. At top, the casts used for securing the forearm and lower leg is shown. **b**, **c**, and **d**, The procedure for HR-pQCT analysis requires a 'scout view' x-ray of the radius or tibia (left) so that the operator can select the region of interest for scanning (solid green bar). Subsequently, three-dimensional data can be obtained in the scan region (right). **e**, A typical section from HR-pQCT showing the ultradistal tibia and fibula. The green line on the periosteal surface of the tibia is used to extract the bone of interest for subsequent three-dimensional analysis

($r^2$=0.73) [24] and cortical porosity ($r^2$=0.80) [28] correlate highly with μCT [28]. Liu et al [29] tested ITS against μCT and found that measurements of HR-pQCT images correlated significantly with those of μCT images at a similar voxel size (80 μm, r=0.71–0.94) and correlations were stronger for plate-related parameters compared with trabecular rods. Tjong et al [1] investigated the impact of different voxel sizes (41, 82, and 123 μm) on HR-pQCT accuracy and found that the 41 μm voxel size correlated best with the μCT measures and the 123 μm voxel size worst for trabecular microstructure and cortical porosity measures. Trabecular density and cortical thickness measures were strongly correlated with μCT across all voxel sizes.

When compared with the gold-standard μCT, HR-pQCT provides moderate to good accuracy in assessing bone structural indices in the radius and tibia.

### *Reproducibility*

Essential to any clinical measurement is the demonstration that measures are reproducible. BMD assessment by HR-pQCT is highly reproducible, with precision errors generally below 1 % [4, 5, 12, 22•]. Structural measures, not surprisingly, have higher precision errors associated with them, ranging from 2.5 %–6.3 % [4, 5, 12, 22•]. FEA intrinsically incorporates a composite of BMD and structural data and has a precision error between that of its components (<3.5 %) [4].

HR-pQCT measures performed at the radius consistently have worse precision than those at the tibia [5, 22•] and in vivo measures have a higher precision error than those ex vivo (ex vivo 0.5 %–1.5 %) [4], both likely owing to greater movement artefacts in the radius (a site easily affected even by the slightest movement of the head, neck, shoulder, arm, or fine tremors of the hand).

Initial work to characterize multi-center precision has begun through a consortium of HR-pQCT centers using anthropomorphic phantoms incorporating cadaveric radii [2•]. Using these phantoms, the ex vivo multi-center precision error across nine HR-pQCT systems was found to be <3 % for density measures and 4 %–5 % for trabecular structure measures. These data will be the basis for testing and validating cross-calibration techniques in the future. Improved automation of all aspects of data acquisition, analysis, and quality assurance will also be integral to multi-center standardization.

### *Segmentation*

When analyzing bone, there are generally two bone compartments considered: cortical and trabecular. At the transitional zone, the confluence of these two compartments, there is little in the way of clear defining borders, presenting a significant challenge [30]. The standard analysis protocol involves the

**Table 1** HR-pQCT parameters with units

| | Abbreviation | Description | Standard unit |
|---|---|---|---|
| Metric measures | | | |
| Total volume | TV | Volume of entire region of interest | $mm^3$ |
| Bone volume | BV | Volume of region segmented as bone | $mm^3$ |
| Bone surface | BS | Surface area of the region segmented as bone | $mm^2$ |
| Bone volume ratio* | BV/TV | Ratio of bone volume to total volume in region of interest | % |
| Bone surface ratio | BS/BV | Ratio of bone surface area to bone volume | % |
| Trabecular thickness* | Tb.Th | Mean thickness of trabeculae | mm |
| Trabecular thickness SD | Tb.Th.SD | Measure of homogeneity of trabecular thickness | mm |
| Trabecular separation* | Tb.Sp | Mean space between trabeculae | mm |
| Trabecular separation SD | Tb.Sp.SD | Measure of homogeneity of trabecular spacing | mm |
| Trabecular number* | Tb.N | Mean number of trabeculae per unit length | per mm |
| Cortical thickness (original)* | Ct.Th | Average cortical thickness | mm |
| Cortical porosity | Ct.Po | Cortical porosity | % |
| Bone mineral density (D100)* | BMD | Total volumetric density | mg $HA/cm^3$ |
| Cortical bone mineral density (Dcomp)* | Ct.BMD | Cortical volumetric density | mg $HA/cm^3$ |
| Trabecular bone mineral density (Dtrab)* | Tb.BMD | Trabecular volumetric density | mg $HA/cm^3$ |
| Total bone area* | Tt.Ar | Cross-sectional area | $mm^2$ |
| Non-Metric Measures | | | |
| Structural model Index | SMI | Measure of trabecular structure (0 for plates and 3 for rods | |
| Degree of anisotropy | DA | 1 is isotropic, >1 is anisotropic by definition; DA = length of longest divided by shortest mean intercept length vector | |
| Connectivity density | Conn.D | Extent of trabecular connectivity normalized by TV | $mm^{-3}$ |
| Cross-sectional moment of inertia | Imin, Imax | minimum and maximum moments of inertia | $mm^4$ |

*Standard HR-pQCT measures are indicated

user manually defining the periosteal surface of the tibia or radius on each slice and a semi-automated contouring algorithm enables this manual process to be typically completed within five minutes. Subsequently, the analysis continues with a filtering and threshold approach that segments the cortical and trabecular bone compartments so that individual compartment analyses can be made. Typically this segmentation process has difficulties in properly identifying the cortex in cases where it is thin or highly porous.

A dual-threshold approach was introduced to address the challenge of bone compartment segmentation. This approach employs a series of fully-automated image processing steps and has proven to be in excellent agreement with hand-contouring of μCT images of the same bones (r=0.9 to 1.0) [19]. This dual-threshold approach was further improved in a collaboration between the manufacturer and researchers in Calgary and San Francisco and is now available as part of the software package for all users of HR-pQCT [22•].

Alternative segmentation approaches have recently been proposed, including a threshold-independent segmentation tool that was shown to have a high degree of agreement with hand-contouring [20]. Most recently, another method that bases segmentation (and cortical porosity measurements) on a density profile analysis across the cortex [21•], may also allow for the identification of the transitional zone [30] between the cortical and trabecular compartments. Currently, both of these methods are implemented on third party platforms and therefore require data conversion and transfer procedures.

## Heterogeneity in Bone Structure in Population Studies

### *Changes with Age*

An important development for HR-pQCT adoption is the establishment of normative databases that provide age- and sex-specific reference data to allow comparison of individual subject data to population-level variation. Normative databases help with the clinical interpretation of HR-pQCT data by allowing for the production of reports that provide context to an individual's HR-pQCT results. It also provides information about the changes in bone microarchitecture as a function of sex and age (albeit from cross-sectional studies of populations). To date there have been three main population-based HR-pQCT studies that have described age-related variation in bone microarchitecture – the

Calgary cohort of the Canadian Multicentre Osteoporosis Study (CaMOS) cohort, the Rochester, Minnesota cohort and the Cambridge, UK cohort [31••, 32, 33]. Table 2 details the changes in HR-pQCT parameters over age.

During puberty, there is a general increase in cortical BMD and a decrease in cortical porosity with a corresponding increase in estimates of bone strength in both sexes [34, 35]. It has also been suggested that transient increases in cortical porosity coincide with the age of highest fracture incidence, during early puberty [36]. With the exception of early puberty, young men have a higher estimated load-to-strength ratio (estimated failure load divided by fall force), or in other words, lower estimated fracture risk.

After puberty, total bone area tends to increase with age, with men generally possessing a larger cross-sectional area compared with women (~33 % larger) [31••]. Postmenopausal women have larger intracortical and endocortical bone surface area compared with premenopausal women [37]. Cortical thickness is higher in men than in women, but declines in both sexes with age and over the menopause [12, 32]. Cortical porosity is higher in young men, but increases with age and after menopause in women [28, 31••, 38•]. In dual energy x-ray absorptiometry (DXA)-assessed areal bone mineral density (aBMD)-matched populations of young (<50 years) and elderly (>50 years) women and men cortical porosity measures alone showed age-related increases (approximately +90 % and +30 % for women and men, respectively) [39].

Young men tend to have similar or greater numbers of trabeculae that are thicker compared with young women [31••, 32, 33]. This results in a greater trabecular bone volume/tissue volume (BV/TV) in young men compared with young women (20–29 years) [33]. Changes after young adulthood have been described as loss of trabecular number and thickness in both genders with aging [31••], decreases in trabecular number only in women with aging and relatively larger losses in trabecular thickness in men [33] and no change in either parameter with age [32]. Postmenopausal women have lower trabecular number compared with premenopausal women [12, 37].

As measured by FEA, young men have stronger bones than young women (34 % to 47 % greater) but both sexes have losses in strength with aging [31••, 32]. The percentage of load carried by trabecular bone increases with aging in both sexes [32] and increases in cortical porosity have shown through FEA to be important determinants of strength [38•]. Load-to-strength ratios tend to increase more in women than in men with aging (27 % more) [31••].

### *Differences in Relation to aBMD*

Osteopenic and osteoporotic women (defined by aBMD) generally have weaker bone in almost all parameters assessed by

**Table 2** Heterogeneity in bone structure in population studies — changes over age and between sexes (all cross-sectional studies)

| Author year [reference] | Ages (y) | f/m | Volumetric bone density changes | Cortical compartment structural changes | Trabecular compartment structural changes |
|---|---|---|---|---|---|
| Liu 2010 [77] | 9–21 | 172/151 | BMD & Ct.BMD ↑ over puberty in f & m | Large ↑ in Ct.Th over puberty in f & m | Tb.Th ↑ in f & m over puberty; little change in Tb.N |
| Nishiyama 2012 [34] | 9–22 | 212/186 | More mature ↑ Ct.BMD | More mature ↓ Ct.Po | m ↑ BV/TV & ↑ Ct.Ar vs f |
| Boutroy, 2005 [12] | 19–88 | 256 | PM f ↓ BMD, Ct.BMD & Tb.BMD vs pre-menopausal f | PM f ↓ Ct.Th vs pre-menopausal f | PM ↓ Tb.Nb & Tb.Th vs pre-menopausal f |
| Nishiyama 2010 [28] | 19–99 | 280/0 | PM f ↓ Ct.BMD vs pre-menopausal f | PM f ↑ Ct.Po; Ct.Th was similar in PMf and pre-menopausal f | N/R |
| Burghardt 2010 [38•] | 20–78 | 94/57 | BMD & Ct.BMD & in f & m; PM f ↓ To.BMD & Ct.BMD vs pre-menopausal | m ↑ Ct.Th vs f; Co.Po increased with age in m & f, but more so in f | N/R |
| Dalzell 2009 [32] | 20–79 | 74/58 | Tb.BMD ↓ f vs m; BMD, Tb.BMD & Ct.BMD all ↓ with age | Ct.Th ↓ in f vs m and loss faster over age in f | m ↑ Tb.N & Tb.Th vs f; no relationship between age and change in trabecular structure |
| MacDonald, 2011 [31••] | 20–99 | 442/202 | BMD & Ct.BMD ↓ in f & m; decreased faster in f | Tt.Ar ↑ through adulthood; ~33 % ↑ young m vs young f | m ↑ Tb.N & Tb.Th vs f; over aging both ↓ Tb.Nb & Tb.Th |
| Khosla 2006 [33] | 21–97 | 324/278 | Ct.BMD ↑ young f than m, but decreased faster in f with aging (22 vs 16 %) | Ct.Th ↓ faster in f with aging vs m (52 vs 38 %, $p=0.001$) | young m ↑ Tb.BV (26 %) & Tb.Th (28 %) vs f; Tb.Nb ↓ with age in f but not in m; Tb.Th ↓ more in men with age vs f |
| Bjornerem 2011 [37] | 40–61 | 185/0 | N/R | PM f ↑ Ct.Po & ↓Ct.Ar vs premenopausal f | PM f ↓ Tb.N & BV/TV vs premenopausal f |

*BMD* Total BMD, *BV/TV* trabecular bone volume/total volume, *Ct.Ar* cortical bone area, *Ct.BMD* Cortical BMD, *Ct.Th* Cortical thickness, *Ct.Po* cortical porosity, *f* female, *m* male, *N/R* Not reported, *PM* postmenopausal, *Tb.BMD* trabecular BMD, *Tb.Nb* trabecular number, *Tb.Th* trabecular thickness, *Tt.Ar* total bone area

HR-pQCT when compared with women with normal aBMD [18, 28]. Areal (DXA-estimated) BMD is higher in men than in women, and declines with age [32] and through menopause [12]. However, not all studies have found an age-associated decline in volumetric BMD by HR-pQCT [38•].

Individuals with similar DXA-based aBMD can have vast differences in results determined by HR-pQCT. Substantial variation in indices reflecting density, structure, and biomechanical competence exist among subjects with identical aBMD results [40]. This could be attributable to differences in bone structure, measurement site, artifacts, or measurement methodology.

## Role of HR-pQCT for Fracture Risk Assessment

HR-pQCT has been demonstrated to be able to discern between women and men with and without fractures. The inherent strength of HR-pQCT is its ability to assess a large slice of bone in three-dimensions for differences in cortical and trabecular characteristics and to identify those characteristics that are most associated with bone weakness, by FEA bone strength modelling.

When compared with DXA aBMD, HR-pQCT measures have a better discriminatory ability to discern between women with and without fractures [16, 41•, 42–44, 45•, 46–48, 49••], even those with similar aBMD [50, 51•]. Differences in HR-pQCT assessed cortical thickness and porosity, BMD, and decay in trabeculae explain a lot of the discriminatory ability. While HR-pQCT bone quality measures are particularly sensitive to discriminate forearm fractures from controls [16, 41•], vertebral fractures appear to be more strongly associated with poor bone quality compared with non-vertebral fractures in general [52–54]. Many of these measures are independent of those assessed by DXA [43, 44].

Ex-vivo examinations comparing DXA and HR-pQCT have concluded that aBMD was highly correlated with BMD and a number of HR-pQCT-obtained microstructural parameters [55]. When combining a DXA-calculated polar moment of inertia measure with aBMD the prediction of specimen structural failure was similar to that obtained by the HR-pQCT measures.

Overall, there is emerging evidence that HR-pQCT is generally superior to DXA for discriminating men and women with and without fractures, especially at the sites of measure (ie, distal radius), although all studies to date were cross-sectional.

### Finite Element Analysis Modeling

Many fractures occur in individuals with normal or osteopenic aBMD, and not only in individuals with aBMD in the osteoporotic range. While density is a reasonable surrogate for bone strength, the assessment of bone mechanical properties by FEA may improve identification of those at high risk for fracture because it provides a more comprehensive measure of bone strength based on both bone microarchitecture and BMD of each tiny element from the three-dimensional image. FEA parameters at the radius and tibia are associated with all types of fragility fractures in both men [56•] and women [57].

FEA modeling has also been shown to accurately predict the energy needed for fracture in ex vivo studies. At the wrist, FEA models have correlated highly with bone stiffness ($r^2$=0.79) and strength ($r^2$=0.87–0.96) obtained with mechanical testing [58–60]. In many of these models, the zones that display high strains are those where fracture subsequently occurred [58].

Emerging FEA approaches include the use of accelerated computational performance based on either multiple central processing unit cores, or even multiple graphics processing unit cores. It is now possible with some software applications to analyze a typical HR-pQCT scan on standard consumer workstations in under two minutes, compared with hours on less-optimized systems [61].

## Role of HR-pQCT in Monitoring Therapy

There are current limitations to the use of DXA in monitoring osteoporosis therapies. The percent of fracture risk reduction attributable to changes in aBMD with different therapies varies from 5 % to 85 % [62–66]. HR-pQCT presents the potential to monitor other components of bone strength, with possibly greater discrimination between different osteoporosis therapies. Thus, the interest in applying HR-pQCT to clinical research studies has grown significantly in recent years, and data from recent studies have provided interesting insights into the effect of new and existing osteoporosis therapies on bone structure and strength.

Treatment with alendronate over one and two years largely preserves BMD, cortical thickness, trabecular BV/TV, and estimated failure load [67, 68, 69••]. One study found that after two years of alendronate therapy there were significant improvements in BMD, cortical thickness and cortical area at the distal tibia, but not at the radius [70]. Treatment with zoledronic acid for 18 months significantly increased total BMD, cortical BMD, cortical thickness, and trabecular BV/TV at both sites, but had no impact on cortical porosity [71]. FEA revealed maintenance of bone strength with zoledronic acid therapy. After two years of ibandronate therapy, there was no change in trabecular bone microarchitecture, however at the tibia there was a preservation of cortical thickness and gains in cortical BMD [72]. One year of treatment with denosumab resulted in maintenance or increases in total, cortical, and trabecular BMD and cortical thickness [69••].

One year of strontium ranelate therapy increased trabecular BMD, cortical thickness, and cortical area [68]. Two years of treatment with strontium ranelate resulted in increases in cortical BMD, cortical thickness, trabecular BV/TV, and FEA-estimated failure load [67]. These data may be affected by beam hardening from the artifact of the higher atomic number of strontium compared with calcium incorporated in bone.

Odanacatib therapy has been shown to increase total, cortical, and trabecular BMD as well as increase cortical thickness at both the radius and the tibia after two years of therapy [73]. FEA demonstrated an increase in the estimated failure load (increased bone strength) at both sites with odanacatib therapy over two years.

Teriparatide therapy for 18 months results in decreases in total BMD, cortical BMD, and cortical thickness with concomitant increases in cortical porosity [71, 74]. Teriparatide therapy was also associated with trabecular thinning, an increase in trabecular number and reduced trabecular BV/TV at the wrist [71]. Despite these changes in bone quality, bone strength was maintained over the 18-month follow-up [71, 74]. With PTH 1-84 there is a loss of estimated bone strength at the radius and tibia strength after 18 months of therapy [71].

## Limitations and Challenges of HR-pQCT

It is important to recognize that HR-pQCT only assesses bone at two sites of the peripheral skeleton typically, and there is a concern whether measurements at these sites reflect strength at the axial skeleton (ie, hip and spine). There is limited data, but the few studies that have examined the relationship between HR-pQCT measurements of the peripheral skeleton have shown a moderate correlation (r=0.56–0.70) to the axial skeleton [75, 76]. Furthermore, it is important to emphasize that the radius itself is an important fracture site, and certainly there is no better imaging technology available than HR-pQCT to measure bone structure at that site. The value of the tibial measurement in relation to fracture is less directly relevant, but the value of having a tibial measurement is that it is a weight-bearing site, as opposed to the radius. Lastly, evidence is still emerging as to whether the distal radius (or tibia) is a responsive skeletal site for monitoring therapy; however, evidence based on the clinical trials conducted to date are encouraging (as noted above).

Segmentation is a continuing challenge, and a focus of much energy in technology development. Despite the fact that HR-pQCT is the highest resolution in vivo scanner available for human bone measurements, the 82 μm voxel size poses challenges in segmentation because a human trabeculae is close in physical dimension. In addition, direct quantification of porosity is limited to relatively large Haversian canals that are resolvable by HR-pQCT. Furthermore, identifying the delineation between the cortical and trabecular compartments is challenging, largely because a precise border is not always present due to real biological effects in the endocortical and intracortical envelopes. Various strategies have been developed, as discussed earlier, but the most crucial aspect is the reproducibility rather than the accuracy of the segmentation process. Removing operator bias has the advantage of producing more reproducible data, as well as ensuring consistency among HR-pQCT centers. Nevertheless, this is an area of HR-pQCT methodology that requires more work.

There are several other technical issues, such as the partial volume effect, beam hardening, and assumptions in the calculations of all the structural and densitometric measures. While not all of these errors can be corrected, it is important to recognize that they exist and interpret the findings accordingly. For example, measures such as the structural model index, which is highly sensitive to image resolution, should be interpreted with caution when derived from HR-pQCT, because it is highly sensitive to motion artifacts, which can occur especially when scanning the radius. Density-based measures may be susceptible to beam hardening and scatter artifacts.

## Conclusions

HR-pQCT provides unprecedented ability to measure human bone microarchitecture at the wrist and ankle in the clinical setting, and these data are providing new insight into changes in bone quality across the lifespan as well as the impact of anti-osteoporosis therapies on bone quality. Before this cutting edge research tool can be used in routine clinical practice, it is imperative to show its utility for fracture prediction, either in conjunction with DXA-based aBMD or in lieu of DXA. While today HR-pQCT is strictly a research tool, it is a relatively easy technology to utilize in the ‘standard analysis’ or automatic analysis default mode, thus opening the possibility for wider use in the hands of ‘non experts’. If it can be demonstrated that HR-pQCT provides value to bone quality assessment, the currently prohibitive cost of the systems would likely be substantially decreased as production increases. Currently, there are less than 45 HR-pQCT systems world-wide, compared with thousands of DXA machines. With the development of normative databases, it will be possible to provide better context of the outcome measures from HR-pQCT, similar in concept to the T-scores that are routine outputs from DXA scan reports. Fracture risk assessment (such as FRAX) could potentially be adapted to include HR-pQCT parameters.

In summary, the three-dimensional measurement of bone by HR-pQCT confers significant advantages over two-dimensional measurements based on DXA. It provides assessment of not only BMD, but also of bone structure and strength. To fully realize the potential of this technology for clinical use, many more clinical studies in different populations will need to be performed.

**Disclosure** AM Cheung has a consultancy with Amgen, Eli Lilly, Merck, Novartis, and Warner Chilcott; has received payment for lectures with Amgen, Eli Lilly, and Warner Chilcott; and institution has grants with Amgen, Eli Lily, and Merck. JD Adachi has a board membership and has received payment for development of education presentations from Amgen, Eli Lilly, Merck, and Novartis; and has a consultancy, grants, and received payment for lectures from Amgen, Eli Lily, Merck, Novartis, and Warner Chilcott. DA Hanley is on the advisory board for Amgen Canada, Eli Lilly Canada, Novartis Canada, and Merck Canada; has received lecture payments from Amgen Canada, Eli Lilly Canada, Novartis Canada, Warner Chilcott, and Merck; institution has received grants from Amgen, Eli Lilly, Merck, Novartis, Canadian Institutes of Health Research, and NPS Pharmaceuticals. DL Kendler has received grants from Pfizer, Amgen, Eli Lilly, Novartis, Johnson & Johnson, and GSK; has received a consulting fee from Pfizer, Amgen, Eli Lilly, Novartis, GSK, Warner Chilcott, and Merck; has received support for travel to meetings from Amgen, Merck, Novartis, and Eli Lilly; and has received fees for participation in review activities from Merck. KS Davison has received a consulting fee and board membership from Amgen and Merck; has received payment for lectures from Amgen, Merck, Novartis, and Warner Chilcott; payment for manuscript preparation from Amgen and Novartis, payment for development of educational presentations from Amgen, Warner Chilcott, and Merck; and support for travel from Amgen. R Josse has a board membership, has received a consulting fee, and payment for lectures from Merck, Lilly, Amgen, and Novartis; has received grants from Amgen. JP Brown has a board membership with Amgen, Eli Lilly, and Merck; has a consultancy with Amgen, Eli Lilly, Merck, and Novartis; has received payment for lectures from Amgen, Eli Lilly, and Novartis; and institution has grants with Warner Chilcott, Novartis, Merck, Eli Lilly, and Amgen. LG Ste-Marie has a board membership with Alliance for Better Bone Health, Warner Chilcott & Sanofi Aventis, Merck, Paladin, Amgen, Novartis, Eli Lilly, and Servier; is a consultant for Europharm and Yoplait; has received payment for lectures from Amgen, Novartis, Warner Chilcott, Eli Lilly, Genzyme, Merck, Paladin, Servier, and Shire; and his institution has grants/grants pending with Alliance for Better Bone Health, Amgen, Novartis, Warner Chilcott, Eli Lilly, Genzyme, Pfizer, and Servier. R Kremer is a consultant for Amgen; has received grants from CIHR and Komen; has received payment for lectures from Amgen and Lilly; and has received payment for development of educational presentations from Amgen and Lilly. MC Erlandson declares no conflicts of interest. L Dian declares no conflicts of interest. AJ Burghardt is on the advisory board for Amgen; and institution has a grant with NIH/NIAMS (NIH R01 AR060700 ). SK Boyd declares no conflicts of interest.



## References

Papers of particular interest, published recently, have been highlighted as:

- • Of importance
- •• Of major importance

1. Tjong W, Kazakia GJ, Burghardt AJ, Majumdar S. The effect of voxel size on high-resolution peripheral computed tomography measurements of trabecular and cortical bone microstructure. Med Phys. 2012;39:1893–903.
2. • Burghardt AJ, Pialat JB, Kazakia GJ, et al. Multicenter precision of cortical and trabecular bone quality measures assessed by high-resolution peripheral quantitative computed tomography. J Bone Miner Res. 2013;28:524–36. *Provides first data on multicenter data comparability, long term precision, and scanner spatial resolution and noice performance based on bone phantom measurements performed at nine different HR-pQCT systems*.
3. Sekhon K, Kazakia GJ, Burghardt AJ, et al. Accuracy of volumetric bone mineral density measurement in high-resolution peripheral quantitative computed tomography. Bone. 2009;45:473–9.
4. MacNeil JA, Boyd SK. Improved reproducibility of high-resolution peripheral quantitative computed tomography for measurement of bone quality. Med Eng Phys. 2008;30:792–9.
5. Engelke K, Stampa B, Timm W, et al. Short-term in vivo precision of BMD and parameters of trabecular architecture at the distal forearm and tibia. Osteoporos Int. 2012;23:2151–8.
6. Pialat JB, Burghardt AJ, Sode M, et al. Visual grading of motion induced image degradation in high resolution peripheral computed tomography: impact of image quality on measures of bone density and micro-architecture. Bone. 2012;50:111–8.
7. Sode M, Burghardt AJ, Pialat JB, et al. Quantitative characterization of subject motion in HR-pQCT images of the distal radius and tibia. Bone. 2011;48:1291–7.
8. • Pauchard Y, Liphardt AM, Macdonald HM, et al. Quality control for bone quality parameters affected by subject motion in high-resolution peripheral quantitative computed tomography. Bone. 2012;50:1304–10. *In multicenter trials, controlling for motion artifact is important and to ensure there is a consistent level of control at each site This study introduces a quantitative approach to measure motion artifact that can be used for quality control*.
9. Pauchard Y, Ayres FJ, Boyd SK. Automated quantification of three-dimensional subject motion to monitor image quality in high-resolution peripheral quantitative computed tomography. Phys Med Biol. 2011;56:6523–43.
10. Pauchard Y, Boyd SK. Landmark based compensation of patient motion artefacts in computed tomography. Proc SPIE Med Imaging. 2008;6913:69133C-1–69133C-10.
11. Shi L, Wang D, Hung VW, et al. Fast and accurate 3-D registration of HR-pQCT images. IEEE Trans Inf Technol Biomed. 2010;14:1291–7.
12. Boutroy S, Bouxsein ML, Munoz F, Delmas PD. In vivo assessment of trabecular bone microarchitecture by high-resolution peripheral quantitative computed tomography. J Clin Endocrinol Metab. 2005;90:6508–15.
13. Laib A, Hauselmann HJ, Ruegsegger P. In vivo high resolution 3D-QCT of the human forearm. Technol Health Care. 1998;6:329–37.
14. Laib A, Ruegsegger P. Comparison of structure extraction methods for in vivo trabecular bone measurements. Comput Med Imaging Graph. 1999;23:69–74.
15. Hildebrand T, Ruegsegger P. Quantification of bone microarchitecture with the structure model index. Comput Methods Biomech Biomed Eng. 1997;1:15–23.
16. Atkinson EJ, Therneau TM, Melton III LJ, et al. Assessing fracture risk using gradient boosting machine (GBM) models. J Bone Miner Res. 2012;10. doi:10.1002/jbmr.1577.
17. Odgaard A, Gundersen HJ. Quantification of connectivity in cancellous bone, with special emphasis on 3-D reconstructions. Bone. 1993;14:173–82.
18. Liu XS, Cohen A, Shane E, et al. Individual trabeculae segmentation (ITS)-based morphological analysis of high-resolution peripheral quantitative computed tomography images detects abnormal trabecular plate and rod microarchitecture in premenopausal women with idiopathic osteoporosis. J Bone Miner Res. 2010;25:1496–505.
19. Buie HR, Campbell GM, Klinck RJ, et al. Automatic segmentation of cortical and trabecular compartments based on a dual threshold technique for in vivo micro-CT bone analysis. Bone. 2007;41:505–15.

20. Valentinitsch A, Patsch JM, Deutschmann J, et al. Automated threshold-independent cortex segmentation by 3D-texture analysis of HR-pQCT scans. Bone. 2012;51:480–7.
21. • Zebaze R, Zadeh AG, Mbala A, Seeman E. A new method of segmentation of compact-appearing, transitional, and trabecular compartments and quantification of cortical porosity from high resolution peripheral quantitative computed tomographic images. Bone. 2013. (in press). *Description of a new method to segment cortical and trabecular compartments and estimate cortical porosity. Unique in proposing to identify a transition zone, dinstinct from the compact cortex and cancellous bone compartments*.
22. • Burghardt AJ, Buie HR, Laib A, et al. Reproducibility of direct quantitative measures of cortical bone microarchitecture of the distal radius and tibia by HR-pQCT. Bone. 2010;47:519–28. *Description of a method increasingly used at a number of HR-pQCT centers to analyze cortical bone geometry and microstructure, including cortical porosity, which has been a focus of several notable findings in the recent literature*.
23. Barnabe C, Szabo E, Martin L, et al. Quantification of small joint space width, periarticular bone microstructure and erosions using high-resolution peripheral quantitative computed tomography in rheumatoid arthritis. Clin Exp Rheumatol. 2013. In press.
24. MacNeil JA, Boyd SK. Accuracy of high-resolution peripheral quantitative computed tomography for measurement of bone quality. Med Eng Phys. 2007;29:1096–105.
25. Liu XS, Zhang XH, Sekhon KK, et al. High-resolution peripheral quantitative computed tomography can assess microstructural and mechanical properties of human distal tibial bone. J Bone Miner Res. 2010;25:746–56.
26. Varga P, Zysset PK. Assessment of volume fraction and fabric in the distal radius using HR-pQCT. Bone. 2009;45:909–17.
27. Burghardt AJ, Kazakia GJ, Majumdar S. A local adaptive threshold strategy for high resolution peripheral quantitative computed tomography of trabecular bone. Ann Biomed Eng. 2007;35:1678–86.
28. Nishiyama KK, Macdonald HM, Buie HR, et al. Postmenopausal women with osteopenia have higher cortical porosity and thinner cortices at the distal radius and tibia than women with normal aBMD: an in vivo HR-pQCT study. J Bone Miner Res. 2010;25:882–90.
29. Liu XS, Shane E, McMahon DJ, Guo XE. Individual trabecula segmentation (ITS)-based morphological analysis of microscale images of human tibial trabecular bone at limited spatial resolution. J Bone Miner Res. 2011;26:2184–93.
30. Zebaze RM, Ghasem-Zadeh A, Bohte A, et al. Intracortical remodelling and porosity in the distal radius and post-mortem femurs of women: a cross-sectional study. Lancet. 2010;375:1729–36.
31. •• Macdonald HM, Nishiyama KK, Kang J, et al. Age-related patterns of trabecular and cortical bone loss differ between sexes and skeletal sites: a population-based HR-pQCT study. J Bone Miner Res. 2011;26:50–62. *A population-based study that provides not only information about microarchitectural changes across the age-spectrum and for both sexes, but also a basis to compare individual results with a normative population. It is the basis for developing normative reports that are used now at some HR-pQCT measurement sites to provide reference data for comparison with individual results*.
32. Dalzell N, Kaptoge S, Morris N, et al. Bone micro-architecture and determinants of strength in the radius and tibia: age-related changes in a population-based study of normal adults measured with high-resolution pQCT. Osteoporos Int. 2009;20:1683–94.
33. Khosla S, Riggs BL, Atkinson EJ, et al. Effects of sex and age on bone microstructure at the ultradistal radius: a population-based noninvasive in vivo assessment. J Bone Miner Res. 2006;21:124–31.
34. Nishiyama KK, Macdonald HM, Moore SA, et al. Cortical porosity is higher in boys compared with girls at the distal radius and distal tibia during pubertal growth: an HR-pQCT study. J Bone Miner Res. 2012;27:273–82.
35. Burrows M, Liu D, Moore S, McKay H. Bone microstructure at the distal tibia provides a strength advantage to males in late puberty: an HR-pQCT study. J Bone Miner Res. 2010;25:1423–32.
36. Kirmani S, Christen D, van Lenthe GH, et al. Bone structure at the distal radius during adolescent growth. J Bone Miner Res. 2009;24:1033–42.
37. Bjornerem A, Ghasem-Zadeh A, Bui M, et al. Remodeling markers are associated with larger intracortical surface area but smaller trabecular surface area: a twin study. Bone. 2011;49:1125–30.
38. • Burghardt AJ, Kazakia GJ, Ramachandran S, et al. Age- and gender-related differences in the geometric properties and biomechanical significance of intracortical porosity in the distal radius and tibia. J Bone Miner Res. 2010;25:983–93. *This paper presents a population based study that exams the age and sex-related differences in cortical bone, and specifically cortical porosity. Uniquely, it used μFE to specifically determine the mechanical significance of porosity in the cortex across age and genders*.
39. Nicks KM, Amin S, Atkinson EJ, et al. Relationship of age to bone microstructure independent of areal bone mineral density. J Bone Miner Res. 2012;27:637–44.
40. Kazakia GJ, Burghardt AJ, Link TM, Majumdar S. Variations in morphological and biomechanical indices at the distal radius in subjects with identical BMD. J Biomech. 2011;44:257–66.
41. • Nishiyama KK, Macdonald HM, Hanley DA, Boyd SK. Women with previous fragility fractures can be classified based on bone microarchitecture and finite element analysis measured with HR-pQCT. Osteoporos Int. 2012. In press. *Showed that by training a computer model, the microarchitecture and FE bone strength information from HR-pQCT can identify those people with wrist fractures*.
42. Vico L, Zouch M, Amirouche A, et al. High-resolution pQCT analysis at the distal radius and tibia discriminates patients with recent wrist and femoral neck fractures. J Bone Miner Res. 2008;23:1741–50.
43. Sornay-Rendu E, Boutroy S, Munoz F, Delmas PD. Alterations of cortical and trabecular architecture are associated with fractures in postmenopausal women, partially independent of decreased BMD measured by DXA: the OFELY study. J Bone Miner Res. 2007;22:425–33.
44. Sornay-Rendu E, Cabrera-Bravo JL, Boutroy S, et al. Severity of vertebral fractures is associated with alterations of cortical architecture in postmenopausal women. J Bone Miner Res. 2009;24:737–43.
45. • Patsch JM, Burghardt AJ, Yap SP, et al. Increased cortical porosity in type 2 diabetic postmenopausal women with fragility fractures. J Bone Miner Res. 2013;28:313–24. *This study is significant in that it highlights the utility of HR-pQCT to detect mechanically relevant structural effects in a specific fracture population (Type 2 Diabetes) where traditional aBMD has had poor success in predicting fracture.*
46. Ostertag A, Collet C, Chappard C, et al. A case-control study of fractures in men with idiopathic osteoporosis: fractures are associated with older age and low cortical bone density. Bone. 2013;52:48–55.
47. Pialat JB, Vilayphiou N, Boutroy S, et al. Local topological analysis at the distal radius by HR-pQCT: application to in vivo bone microarchitecture and fracture assessment in the OFELY study. Bone. 2012;51:362–8.
48. Boutroy S, Van Rietbergen B, Sornay-Rendu E, et al. Finite element analysis based on in vivo HR-pQCT images of the distal radius is associated with wrist fracture in postmenopausal women. J Bone Miner Res. 2008;23:392–9.
49. •• Melton III LJ, Christen D, Riggs BL, et al. Assessing forearm fracture risk in postmenopausal women. Osteoporos Int. 2010;21:1161–9. *This study is unique among fracture case-*

*control studies in that it recruited exclusively recent forearm fracture subjects (median exam 7 months post-fracture). Furthermore it included a relatively large (N= 100 case, N= 100 control), and racially homogenous study population*.

50. Stein EM, Liu XS, Nickolas TL, et al. Abnormal microarchitecture and reduced stiffness at the radius and tibia in postmenopausal women with fractures. J Bone Miner Res. 2010;25:2572–81.
51. • Liu XS, Stein EM, Zhou B, et al. Individual trabecula segmentation (ITS)-based morphological analyses and microfinite element analysis of HR-pQCT images discriminate postmenopausal fragility fractures independent of DXA measurements. J Bone Miner Res. 2012;27:263–72. *This is a comprehensive study of how HR-pQCT measures of bone density, structure, and strength can discriminate fragility fractures independent of DXA-assessed aBMD*.
52. Szulc P, Boutroy S, Vilayphiou N, et al. Cross-sectional analysis of the association between fragility fractures and bone microarchitecture in older men: the STRAMBO study. J Bone Miner Res. 2011;26:1358–67.
53. Melton III LJ, Riggs BL, Keaveny TM, et al. Relation of vertebral deformities to bone density, structure, and strength. J Bone Miner Res. 2010;25:1922–30.
54. Stein EM, Liu XS, Nickolas TL, et al. Microarchitectural abnormalities are more severe in postmenopausal women with vertebral compared with nonvertebral fractures. J Clin Endocrinol Metab. 2012;97:E1918–26.
55. Popp AW, Windolf M, Senn C, et al. Prediction of bone strength at the distal tibia by HR-pQCT and DXA. Bone. 2012;50:296–300.
56. • Vilayphiou N, Boutroy S, Szulc P, et al. Finite element analysis performed on radius and tibia HR-pQCT images and fragility fractures at all sites in men. J Bone Miner Res. 2011;26:965–73. *This paper is a comparably large case-control study of fracture prevalence in men*.
57. Vilayphiou N, Boutroy S, Sornay-Rendu E, et al. Finite element analysis performed on radius and tibia HR-pQCT images and fragility fractures at all sites in postmenopausal women. Bone. 2010;46:1030–7.
58. Varga P, Baumbach S, Pahr D, Zysset PK. Validation of an anatomy specific finite element model of Colles' fracture. J Biomech. 2009;42:1726–31.
59. Varga P, Pahr DH, Baumbach S, Zysset PK. HR-pQCT based FE analysis of the most distal radius section provides an improved prediction of Colles' fracture load in vitro. Bone. 2010;47:982–8.
60. Varga P, Dall'ara E, Pahr DH, et al. Validation of an HR-pQCT-based homogenized finite element approach using mechanical testing of ultra-distal radius sections. Biomech Model Mechanobiol. 2011;10:431–44.
61. Jorgenson B, Nodwell E, Boyd SK. Acceleration of bone finite element analysis through the use of GPU hardware. Presented at 18th Congress of the European Society of Biomechanics in Lisbon, Portugal. 1-4 July 2012.
62. Ettinger B, Black DM, Mitlak BH, et al. Reduction of vertebral fracture risk in postmenopausal women with osteoporosis treated with raloxifene: results from a 3-year randomized clinical trial. Multiple Outcomes of Raloxifene Evaluation (MORE) Investigators. JAMA. 1999;282:637–45.
63. Black DM, Thompson DE, Bauer DC, et al. Fracture risk reduction with alendronate in women with osteoporosis: the Fracture Intervention Trial. FIT Research Group. J Clin Endocrinol Metab. 2000;85:4118–24.
64. Miller P. Analysis of 1-year vertebral fracture risk reduction data in treatments for osteoporosis. South Med J. 2003;96:478–85.
65. Watts NB, Geusens P, Barton IP, Felsenberg D. Relationship between changes in BMD and nonvertebral fracture incidence associated with risedronate: reduction in risk of nonvertebral fracture is not related to change in BMD. J Bone Miner Res. 2005;20:2097–104.
66. Liberman UA, Hochberg MC, Geusens P, et al. Hip and non-spine fracture risk reductions differ among antiresorptive agents: evidence from randomized controlled trials. Int J Clin Pract. 2006;60:1394–400.
67. Rizzoli R, Chapurlat RD, Laroche JM, et al. Effects of strontium ranelate and alendronate on bone microstructure in women with osteoporosis: results of a 2-year study. Osteoporos Int. 2012;23:305–15.
68. Rizzoli R, Laroche M, Krieg MA, et al. Strontium ranelate and alendronate have differing effects on distal tibia bone microstructure in women with osteoporosis. Rheumatol Int. 2010;30:1341–8.
69. •• Seeman E, Delmas PD, Hanley DA, et al. Microarchitectural deterioration of cortical and trabecular bone: differing effects of denosumab and alendronate. J Bone Miner Res. 2010;25:1886–94. *Data from a double-blind, placebo controlled head-to-head trial of denosumab and alendronate. This study is unique in that it is the first longitudinal HR-pQCT data published and represents one of the only multicenter trials published to date*.
70. Burghardt AJ, Kazakia GJ, Sode M, et al. A longitudinal HR-pQCT study of Alendronate treatment in postmenopausal women with low bone density: relations among density, cortical and trabecular microarchitecture, biomechanics, and bone turnover. J Bone Miner Res. 2010;25:2558–71.
71. Hansen S, Hauge EM, Jensen JE, Brixen K. Differing effects of PTH 1-34, PTH 1-84, and zoledronic acid on bone microarchitecture and estimated strength in postmenopausal women with osteoporosis. An 18 month open-labeled observational study using HR-pQCT. J Bone Miner Res. 2012;10.
72. Chapurlat RD, Laroche M, Thomas T, et al. Effect of oral monthly ibandronate on bone microarchitecture in women with osteopenia-a randomized placebo-controlled trial. Osteoporos Int. 2013;24:311–20.
73. Cheung AM, Burghardt A, Chapurlat R, et al. Imaging and finite element analysis of the spine, hip, radius, and tibia following 2 years of treatment with odanacatib in postmenopausal women. Presented at The International Society for Clinical Densitometry (ISCD) in Tampa, Florida, USA. March 20-23, 2013.
74. Macdonald HM, Nishiyama KK, Hanley DA, Boyd SK. Changes in trabecular and cortical bone microarchitecture at peripheral sites associated with 18 months of teriparatide therapy in postmenopausal women with osteoporosis. Osteoporos Int. 2011;22:357–62.
75. Liu XS, Cohen A, Shane E, et al. Bone density, geometry, microstructure, and stiffness: relationships between peripheral and central skeletal sites assessed by DXA, HR-pQCT, and cQCT in premenopausal women. J Bone Miner Res. 2010;25:2229–38.
76. Cohen A, Dempster DW, Muller R, et al. Assessment of trabecular and cortical architecture and mechanical competence of bone by high-resolution peripheral computed tomography: comparison with transiliac bone biopsy. Osteoporos Int. 2010;21:263–73.
77. Liu D, Burrows M, Egeli D, McKay H. Site specificity of bone architecture between the distal radius and distal tibia in children and adolescents: an HR-pQCT study. Calcif Tissue Int. 2010;87:314–23.